Astron. Astrophys. 162, 21–31 (1986)

ASTRONOMY
AND
ASTROPHYSICS

A base of star clusters for stellar population synthesis*

E. Bica and D. Alloin

Observatoire de Paris, Section de Meudon LAM, F-92195 Meudon Principal Cedex, France

Received May 5, 1985; accepted January 16, 1986

Summary. Integrated spectra of 63 star clusters with 10^6 yr $\leqq$ age $\leqq 1.65\ 10^{10}$ yr and $-2.1 \leqq [Z/Z_\odot] \leqq 0.1$ are presented in this paper. The useful wavelength range 3780, 7690 Å was split into 70 consecutive windows, 24–190 Å wide. The main contributors to the absorption in each window were searched for: apart from the strong well-known absorption features, we detected a number of weaker absorptions quite often due to molecular bands arising from red stars. The equivalent widths W of the spectral features, as well as the continuous distribution are studied as a function of age and metallicity.

Metallic lines and molecular bands present essentially the same behaviour with metallicity. In particular, we show the influence of younger turn-off points on W, for features in the blue part of the spectrum. Indeed, the top main sequence stars then enhance the continuum, defining in the W vs. metallicity plots several loci depending on the age. On the contrary, the W vs. metallicity relationship in the red, tends to be single-valued, regardless of age.

For the windows containing Balmer lines from Hα to Hδ, the age dependence looks similar whatever the line, with a maximum W value for $t \sim 4\ 10^8$ yr. If any, the effect of different metallicities is weak in these windows. For a given age, W(Hα) is always smaller than W(Hβ), W(Hγ) or W(Hδ), due to the fact that its underlying continuum is dominated by late-type stars which contribute very little to the line absorption. For Hε toH10 lines, strongly blended with metallic features, a metal-dominated behaviour is observed.

The continuous distribution of metal-poor globular clusters is strikingly different from that of young blue clusters of any age or metallicity, while their Balmer equivalent widths partly overlap.

These results form a base of star cluster properties which will be used for stellar population synthesis in galaxies. The comparison of W for metallic features in the star clusters and in a sample of 152 nuclei of normal galaxies having types from E to Sc and absolute luminosities M_B from −16.6 to −23.3, shows that around 50 % of the nuclei can be population synthesized with the present cluster base. An extrapolation of the base properties to a metallicity $[Z/Z_\odot] = 0.6$ is required to describe the entire galaxy sample.

Key words: star clusters – spectrophotometry – stellar population synthesis

Send offprint requests to: D. Alloin

* Based on observations collected at the European Southern Observatory, La Silla, Chile

1. Introduction

So far population synthesis in galaxies has been mostly based on spectra of individual stars (Van den Bergh, 1975; Pagel and Edmunds, 1981; Pickles, 1985 and references therein). Some authors used a composite base of stellar spectra and integrated spectra of globular clusters in order to account for possible low metallicity populations in the synthesis (e.g. Faber, 1972; Ciani et al., 1984). The large number of required stellar species and the need for three fundamental parameters (T, g, Z) make difficult the determination of unambiguous solutions, in spite of many plausible astrophysical constraints.

We intend to undertake a different approach to this problem, using *star cluster integrated spectra only*. Therefore a base of 63 star clusters with $-2.1 \leqq [Z/Z_\odot] \leqq 0.1$ and 10^6 yr $\leqq$ age $\leqq 1.65\ 10^{10}$ yr, and of known reddening has been studied. The data consist of low dispersion integrated spectra of Galactic globular clusters, intermediate age red globular clusters as well as blue globular clusters in the Magellanic Clouds (MC), rich and compact Galactic open clusters and H II regions. The main advantage of this method over conventional ones is to reduce the number of variables. A base of stars is essentially described by the temperature, gravity and metallicity. In the case of star clusters, this is reduced to age and metallicity only. Moreover, the number of fundamental species in the cluster base does not need to be as large. Star clusters allow a coverage in metallicity down to a hundreth of solar, while it is observationally difficult to get complete subsets of main sequence and evolved stars with $[Z/Z_\odot] < -0.5$. Finally, this approach is free of any assumption about the initial mass function (IMF) and the details of stellar evolution. Indeed, the integrated spectra of star clusters are built of Nature's exact relative proportions of stars of different masses born from a gas cloud of the corresponding metallicity. As well, the relative proportions of evolved stars as a function of age and metallicity are implicitly the right ones. No assumptions have to be made in that matter.

The choice of the clusters, their distribution in the age vs metallicity plane and the observations are described in the next section. In Sect. 3, we present the spectra in metallicity and age sequences and discuss their main characteristics. Section 4 deals with the selection of the windows, the identification of the contributing absorbers and the analysis of the W and continuum measurements. In view of the population synthesis in galaxies, we derive in Sect. 5 grids of star cluster properties as a function of age and metallicity, and summarize as well the conclusions of this study.

Table 1. Characteristics of the clusters' sample

NAME NGC	AGE 10^7 yrs	$[Z/Z_\odot]$	E(B-V)	AREA 'x'	EXP min	SOURCES
			Small Magellanic Cloud			
121	1200±300	-1.24±0.3	0.03[a]	1x1	60	[3], [5], [6], [10], [19]
330	1.5±0.6	-1.4 ±0.4	"	1x1	20	[3], [6], [7], [15], [19], [32]
419	200±100	-1.2 ±0.3	"	1x1	40	[1], [5], [6], [7], [10], [19]
N 88	<0.2[b]	-0.95[c]	"	0.08x0.22	10	[19], [30], [31]
			Large Magellanic Cloud			
*1466	1400±300	-1.6 ±0.3	0.06[a]	1x0.5	50	[3], [10], [11], [19]
*1714 N4A	0.25±0.05[b]	-0.4[c]	"	1x0.5	10	[19], [31]
1783	300^{+200}_{-100}	-1.0 ±0.5	"	1x1	70	[5], [6], [7], [10], [19], [20]
*1831	30±10	-1.0 ±0.5	"	1x1	30	[5], [6], [7], [19], [22]
*1847	2.5±1.0	-0.25±0.4	"	1x1	26	[6], [19], [25]
*1856	10±3	-0.1 ±0.3	"	1x1	16	[6], [7], [19], [23]
1866	8.6±0.5	-1.2 ±0.2	"	{1x1 1x0.5	{20 20	[6], [7], [15], [16], [19]
1868	50±20	-1.1 ±0.2	"	1x0.5	40	[6], [18], [19]
*1895 N33	0.55±0.05[b]	-0.3[c]	"	1x0.5	30	[19]
1978	200^{+200}_{-100}	-0.8 ±0.4	"	1x0.7	50	[2], [5], [6], [10], [11], [19]
2004	0.8±0.1	-0.25±0.25	"	1x1	20	[6], [19], [20]
2070 30Dor	0.20±0.05	-0.5[c]	"	comp[d]	24	[17], [19], [24], [31]
*2100	1.0±0.2	-0.5 ±0.1	"	1x1	20	[3], [6], [19], [20]
2157	3±2	-0.6 ±0.3	"	1x0.5	20	[6], [15], [19]
2214	4±1	-1.2 ±0.2	"	1x1	30	[6], [7], [15], [19]
			Galactic Globular Clusters			
104 47TUC	1650±150	-0.70±0.15	0.08±0.04	3x3	12	[8], [9], [12], [13], [21]
362	"	-1.25±0.15	0.06±0.02	{1.5x1.5 1x0.5	{20 15	[4], [8], [9], [12], [13], [20]
1851	"	-1.3 ±0.2	0.09±0.02	1x0.5	10	[4], [8], [9], [12], [13]
1904 M79	"	-1.55±0.15	0.00±0.02	{1x0.5 1x1	{20 20	[4], [8], [9], [12], [13]
2808	"	-1.25±0.20	0.21±0.02	2x2	20	[8], [9], [12], [13]
4590 M68	"	-2.00±0.15	0.04±0.02	2x1	40	[4], [8], [9], [12], [13]
4833	"	-1.7 ±0.2	0.31±0.03	1.5x1.5	30	[4], [8], [9], [12], [13]
5024 M53	"	-1.85±0.15	0.01±0.02	2x0.5	30	[4], [8], [9], [12], [13]
5824	"	-1.8 ±0.2	0.12±0.02	1x0.5	10	[8], [9], [12], [13]
5927	"	-0.15±0.15	0.47±0.05	1x0.5	20	[8], [9], [12], [13], [21]
*5946	"	-1.5 ±0.2	0.61±0.07	0.5x0.5	19	[8], [9], [12], [13]
*6093 M80	"	-1.6 ±0.2	0.17±0.03	1x0.5	10	[8], [9], [12], [13]
*6139	"	-1.5 ±0.2	0.70±0.07	1x0.5	16	[8], [9], [12], [13]
6171 M107	"	-0.90±0.15	0.37±0.04	2x2	50	[4], [8], [9], [12], [13], [21]
*6287	"	-1.6 ±0.5	0.5 ±0.1	1x0.5	30	[8], [9], [12], [13]
*6293	"	-1.8 ±0.2	0.36±0.02	1x0.5	16	[8], [9], [12], [13]
*6304	"	-0.2 ±0.4	0.50±0.07	1x0.5	16	[8], [9], [12], [13]
*6316	"	-0.1 ±0.4	0.6 ±0.1	1x0.5	20	[8], [9], [12], [13]
*6356	"	-0.25±0.35	0.27±0.03	1x0.5	30	[8], [9], [12], [13]
*6388	"	-0.6 ±0.2	0.37±0.02	1.5x0.5	10	[8], [9], [12], [13]
*6401	"	-1.1 ±0.2	0.81±0.03	0.5x0.5	32	[8] [12], [13]
6402 M14	"	-1.1 ±0.3	0.55±0.06	2x2	50	[4], [8], [9], [12], [13]
6440	"	0.04±0.3	1.11±0.02	1x05	40	[8], [9], [12], [13]
*6453	"	-1.4 ±0.2	0.61±0.02	0.5x0.5	20	[8], [9], [12], [13]
*6517	"	-1.75±0.4	1.06±0.02	0.5x0.5	20	[8], [9], [12], [13]
*6528	"	-0.05±0.2	0.66±0.09	0.5x0.5	20	[8], [9], [12], [13]
6541	"	-1.65±0.25	0.12±0.05	2x0.5	20	[8], [9], [12], [13]
*6544	"	-1.1 ±0.4	0.72±0.08	0.5x0.5	20	[8], [9], [12], [13]
*6553	1650±150	0.1 ±0.4	0.79±0.09	1x0.5	50	[8], [9], [12], [13]
*6558	"	-1.3 ±0.2	0.40±0.15	0.5x0.5	20	[8], [9], [12], [13]

Table 1 (continued)

NAME NGC	AGE 10^7 yrs	$[Z/Z_\odot]$	E(B-V)	AREA 'x'	EXP min	SOURCES
*6569	"	-0.8 ±0.1	0.59±0.04	1x0.5	30	[8], [9], [12], [13]
*6624	"	-0.3 ±0.2	0.29±0.05	1x0.5	10	[8], [9], [12], [13]
*6637 M69	"	-0.55±0.3	0.18±0.02	1x0.5	16	[8], [9], [12], [13], [21]
*6638	"	-0.95±0.2	0.40±0.02	1x0.5	16	[8], [9], [12], [13]
*6642	"	-1.35±0.2	0.38±0.02	0.5x0.5	14	[8], [9], [12], [13]
*6652	"	-0.6 ±0.3	0.09±0.02	0.5x0.5	18	[8], [9], [12], [13]
*6715 M54	"	-1.25±0.2	0.14±0.02	1x0.5	10	[4], [8], [9], [12], [13]
*6760	"	-0.4 ±0.2	0.85±0.09	1x0.5	28	[8], [9], [12], [13]
6864 M75	"	-1.25±0.15	0.16±0.02	1x0.5	20	[8], [9], [12], [13]
7006	"	-1.45±0.20	0.07±0.05	1x0.5	30	[8], [9], [12], [13]
7078 M15	"	-2.05±0.25	0.08±0.02	2x0.5	20	[4], [8], [9], [12], [13], [20]
			Galactic Open Clusters			
2158	120±50[e]	-0.65±0.25	0.43±0.05	1.5x1.5	90	[14], [27]
2660	120±30	-0.02±0.25	0.38±0.05	1x0.5 1.5x1.5	50 20	[14], [26]
6705 M11	17±5	0.11±0.09	0.42±0.05	2x2	30	[14], [28], [29]

Notes to Table 1

[a] We adopted for homogeneity, a Galactic reddening $E(B-V) = 0.03$ and 0.06 for all objects in the SMC and LMC respectively (Mould and Aaronson, 1980). However, there are indications that both H II regions and some blue star clusters may be reddened (e.g. Hodge and Lee, 1984)

[b] The age determination is based on the $W(H\beta)$ vs. age relationship in H II regions (Dottori, 1981), corresponding to the $5'' \times 13''$ entrance slit

[c] This value is deduced from the oxygen relative abundance

[d] Scans are made of three clumps in the stellar association and of the central emission filaments free of stellar contamination. The emission spectrum was adjusted with the sum of the stellar clumps' spectra so as to reproduce the integrated $H\beta$ equivalent width in a 10′ diaphragm (Dottori and Bica, 1981)

[e] Arp and Cuffey (1962) concluded that the age of NGC 2158 is intermediate between that of the Hyades and NGC 752. The value given here is the mean of recent age determinations for the latter clusters (McClure and Twarog, 1978)

References to Table 1

1 Durand et al. (1984)
2 Olszewski (1984)
3 Hodge (1984a)
4 Smith (1984)
5 Mould and Aaronson (1982)
6 Hodge (1983)
7 Searle et al. (1980)
8 Van den Berg (1983)
9 Bica and Pastoriza (1983)
10 Dottori et al. (1983)
11 Cowley and Hartwick (1982)
12 Janes and Demarque (1983)
13 Zinn and West (1984)
14 Janes (1979)
15 Richtler and Nelles (1983)
16 Becker and Mathews (1983)
17 Boeshaar et al. (1983)
18 Hodge (1982)
19 Mould and Aaronson (1980)
20 Cohen (1982)
21 Cohen (1983)
22 Hodge (1984b)
23 Hodge and Lee (1984)
24 Dottori and Bica (1981)
25 Nelson and Hodge (1983)
26 Hartwick and Hesser (1973)
27 Arp and Cuffey (1962)
28 Mermilliod (1981a)
29 Barbaro et al. (1969)
30 Dufour and Harlow (1977)
31 Pagel et al. (1978)
32 Carney et al. (1985)

2. Choice of the cluster base and observations

The main criterion in the selection of the star clusters was the knowledge of their age, metallicity and reddening. These quantities are listed respectively in columns 2–4 of Table 1, together with their uncertainties taking into account both individual error bars and the discrepancies among different sources which are given in column 7. The metal abundance determinations derived by a variety of methods were grouped under the symbol $[Z/Z_\odot]$, the logarithm of metal content relative to the Sun.

The distribution of the clusters in the plane age vs metallicity is shown in Fig. 1. Metallicities from solar down to $[Z/Z_\odot] \simeq -2$ fill in the plane for essentially all ages, from young clusters about 10^7 yr old to Galactic globular clusters with ages in the range 15 to 18 10^9 yr (Vandenberg, 1983; Janes and Demarque, 1983). The MC clusters allowed the coverage of the intermediate and low metallicity ranges for young and intermediate ages. The Galactic open clusters cover the metal rich young and intermediate ages in the plane. This base offers a wide range of possible chemical evolution models for subsystems in galaxies to be synthesized.

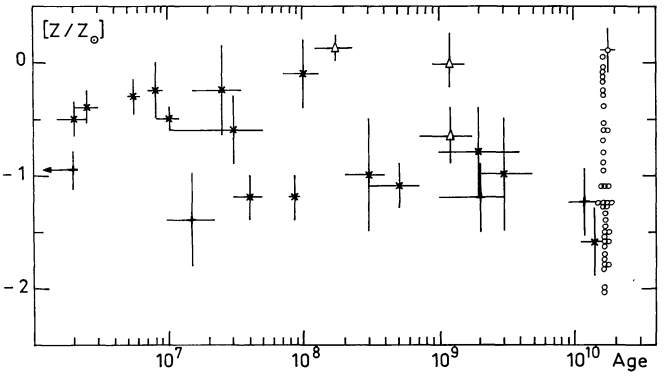

Fig. 1. Distribution of the cluster sample in the age, metallicity plane. For globular clusters, 1650 10^7 yr old, the typical error bar is indicated for one of the points only. Open triangles refer to Galactic open clusters (GOC); open circles to Galactic globular clusters (GGC); crosses and plus signs to the LMC and SMC clusters respectively

The observations were carried out with the IDS attached to the Boller and Chivens spectrograph at the ESO 1.52 m telescope (La Silla). We obtained in January, July and November 1984 and May 1985 integrated spectra of 3 clusters in the SMC, 12 in the LMC, 41 Galactic globular clusters and 3 rich compact Galactic open clusters, as well as of 4 H II regions.

The wide range of cluster angular sizes required different observing techniques in order to get integrated spectra. Larger angular size objects were scanned in declination with the slit height set along right ascension. Moreover several side by side successive exposures were made at different right ascensions. Small compact clusters in the MC demanded only restricted scanning. In column 5 of Table 1, we have listed the area of the cluster seen in our observations. The slit size was $5'' \times 13''$, except in the case of objects with an asterisk in column 1, for which the slit height had been set to $8''$.

Low resolution spectra are particularly suitable for synthesizing stellar populations in galactic nuclei which, quite often, have large stellar velocity dispersions. Therefore, we used a 300 gr/mm grating in the first order providing a mean dispersion of 224 Å mm^{-1} over the range 3700, 8200 Å. A final resolution of 11 Å was achieved, as measured by the mean FWHM of the comparison lines. We provide in column 6 of Table 1, the total effective exposure on each object. These were such as to produce about the same signal to noise ratio for all spectra. Two or three standard stars were observed each night for flux calibration and estimate of the subsequent error-bars. The reductions were made in a convectional way, using the IHAP system at ESO (Garching) and IAP (Paris).

3. Metallicity and age sequences in the cluster base

All cluster spectra have been corrected for reddening using the $E(B-V)$ values from Table 1, a normal reddening law $A_\lambda = 0.65\, A_v(1/\lambda - 0.35)$ and the relation $A_v = 3\,E(B-V)$. They have been normalized relative to the continuum at 5870 Å. Apart from the strong well known absorptions, we detected a number of weaker features. Most of this widespread absorption, seen in clusters of all ages, is due to molecular bands arising in red stars (Sect. 4) and it tends to be underestimated in higher dispersion data, owing to the inclusion of fewer trustworthy maxima.

In Fig. 2, we present the Galactic globular clusters in a downward decreasing metallicity sequence. An obvious enhancement with metallicity appears for strong features such as Ca II K, the G-band, the Mg I triplet, Na I and TiO relative to the continuum height. Metal-rich globular clusters like NGC 5927 and 6528 exhibit lower blue to red continuum ratios. This arises from both the blanketing effect of numerous metallic absorptions towards the blue and the absence of blue horizontal branch stars (BHB). Conversely, the prominent BHB in metal poor clusters like NGC 7078 raises and flattens the blue end of the continuum, as well as strengthening the Balmer lines. The latter effect can easily be seen by comparing the blend Hε + Ca II H to Ca II K.

We have displayed in Fig. 3 a downward increasing age sequence for Magellanic clusters and one moderately metal rich Galactic open cluster. The properties of NGC 121 in the SMC are comparable to those of Galactic halo globular clusters with similar HR diagrams and having RR Lyrae stars (Van den Bergh, 1975 and references therein). The cluster NGC 1978 belongs to the red intermediate age clusters of the MC. The distribution of the integrated $(U-B)_0$ vs. $(B-V)_0$ colors of such clusters deviates from that of Galactic globular clusters (Van den Bergh, 1981), owing mostly to younger ages from 10^9 to 10^{10} yr, as derived from HR diagrams (Hodge, 1983). The integrated spectra of red star clusters from 3800 to 5200 Å have been analyzed by Rabin (1982); near the lower age limit of this class, we show the Galactic open cluster NGC 2158. The LMC cluster NGC 1868, with an integrated color $(B-V) = 0.45$ (Van den Bergh, 1981) is one of the rare objects intermediate between the so-called blue and red Magellanic globular clusters. In the upper part of Fig. 3, we show blue Magellanic clusters together with the giant LMC H II region NGC 2070: the increasing contribution from brighter and bluer turn-offs in younger clusters strengthens the blue part of the integrated continuum. The blue to red continuum ratios for star clusters younger than 10^9 yr (Fig. 3) are larger than those for old metal-poor objects like NGC 7078 (Fig. 2). Thus, the continuum distribution differences and not the Balmer line equivalent widths which partly overlap (Sect. 4) are important for distinguishing between young populations and old metal-poor ones in galaxies.

The effect of intrinsic reddening is easily observed in H II regions (NGC 2070). Together with internal reddening, the effect of rapid stellar evolution around 10^7 yr (NGC 2004) decreases the continuum slope by the development of an important red supergiant population. After this age, the clusters appear to be essentially dust free and as a consequence exhibit then a very blue continuum (Fig. 3).

4. Selected windows and results

Even in the case of individual stars, it is not a simple task to find out from low dispersion spectra, the nature of the numerous weak absorption features. This results obviously from blending effects and from a large number of atomic or molecular lines to be possibly assigned. The composite nature of a cluster spectrum is an additional difficulty in that matter.

The equivalent widths of selected wavelength ranges in the spectra of different clusters are intended to be used in a synthesis, for comparison with the same measurements in the spectra of galaxies. This approach does not require a detailed identification of the absorbers. Consequently the useful wavelength range 3780–7690 Å was split into consecutive windows, 24–190 Å wide. Such widths are suitable for avoiding problems due to possible

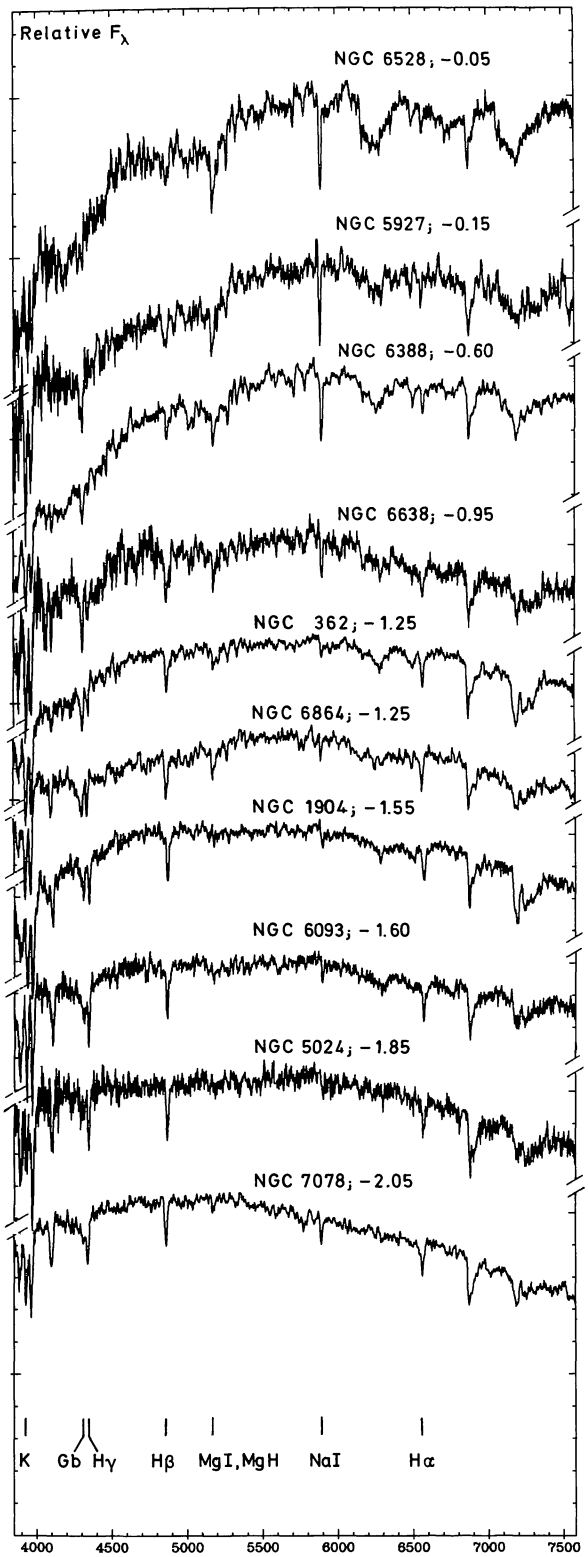

Fig. 2. The metallicity sequence for globular clusters. The spectra are corrected for foreground reddening and are normalized to $F_{5870}=1$

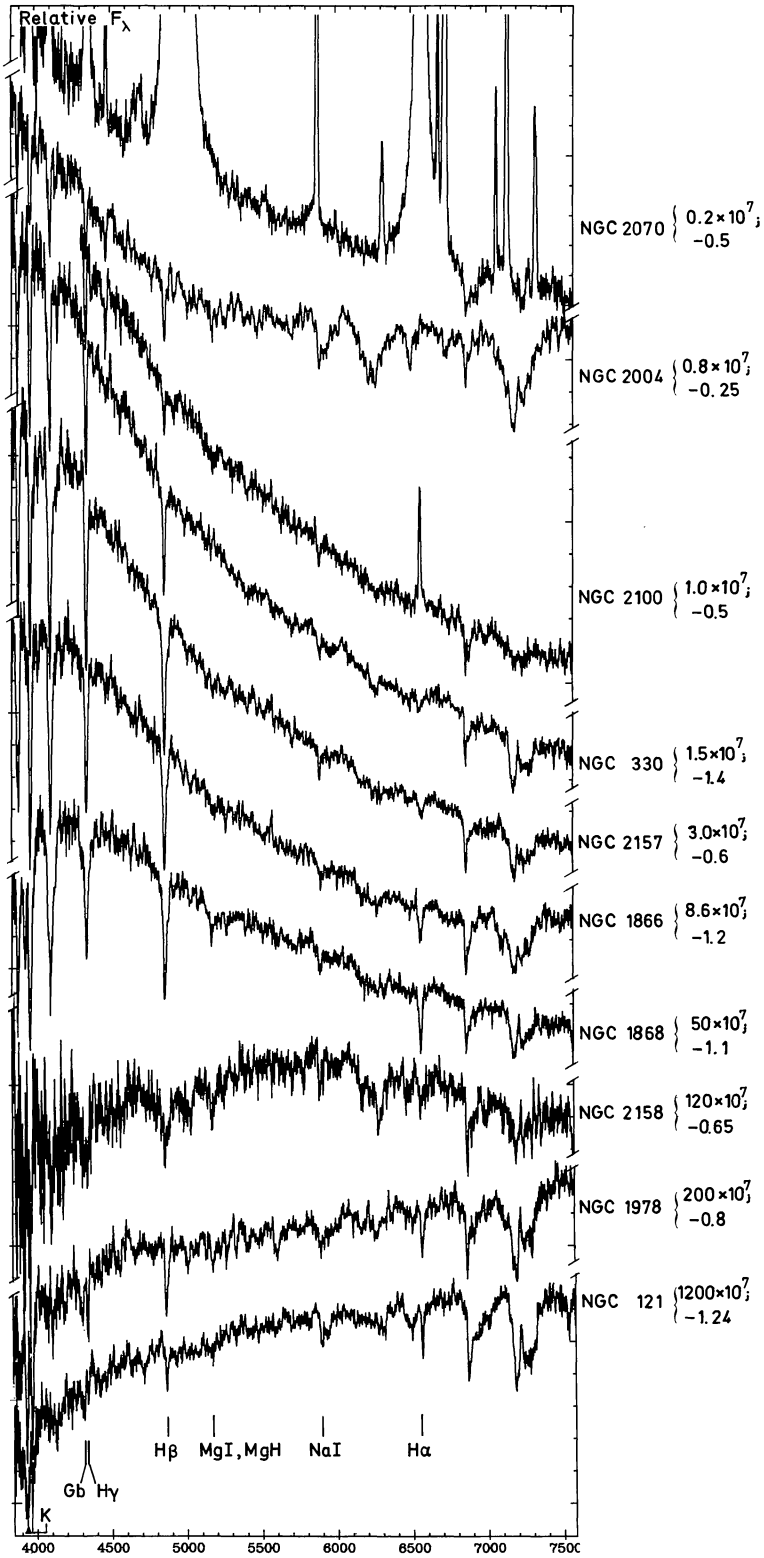

Fig. 3. The age sequence for young clusters. Reddening and normalization as in Fig. 2

Table 2. Window parameters

#	Δλ(Å)	W/Δλ	ABSORBERS
1	3780–3814	0.13	H10 ; CN Lband
2	3814–3862	0.19	H9 ; CN Lband ; FeI ; MgI ; HeI
3	3862–3908	0.18	H8 ; CN Lband ; FeI ; SiI ; HeI
4	3908–3952	0.20	CaII K
5	3952–3988	0.26	CaII H ; Hε
6	3988–4020	0.04	FeI ; HeI
7	4020–4058	0.03	FeI ; HeI
8	4058–4082	0.06	FeI ; SrII
9	4082–4124	0.13	Hδ
10	4124–4150	0.08	FeI
11	4150–4214	0.06	CN
12	4214–4244	0.06	CaI
13	4244–4284	0.07	FeI ; CrI
14	4284–4318	0.14	CH Gband ; FeI ; CrI
15	4318–4364	0.12	Hγ ; FeI ; FeII
16	4364–4420	0.06	FeI ; C_2 ; FeII ; TiII
17	4420–4450	0.06	FeI ; CaI
18	4450–4484	0.04	TiO ; MgII ; CaI ; HeI
19	4484–4510	0.01	CH ; CN
20	4510–4568	0.03	FeI ; BaII ; FeII ; TiII
21	4568–4622	0.02	FeI , TiO ; CaI ; FeII ; TiII ; CN
22	4622–4668	0.02	FeI ; TiO
23	4668–4698	0.02	TiO ; C_2
24	4698–4750	0.02	FeI ; C_2 ; MgI ; TiI ; NiI ; HeI
25	4750–4802	0.03	MgH ; TiO ; FeI ; MnI ; NiI
26	4802–4846	0.03	TiO ; MgH ; CN ; MnI
27	4846–4884	0.11	Hβ ; TiO ; FeI
28	4884–4908	0.04	FeI
29	4908–4950	0.03	FeI ; FeII ; CN ; HeI
30	4950–4998	0.03	FeI ; TiO ; TiI
31	4998–5064	0.04	FeI ; TiO ; CN ; FeII ; TiI ; HeI
32	5064–5130	0.03	FeI ; C_2
33	5130–5156	0.05	MgH ; FeI ; C_2 ; CN
34	5156–5196	0.08	MgI+MgH ; C_2 ; TiO
35	5196–5244	0.04	MgH ; FeI ; CrI ; CN
36	5244–5314	0.03	FeI ; TiO ; CaI ; TiI
37	5314–5364	0.02	FeI ; TiO ; CN ; CaI
38	5364–5420	0.02	FeI ; MnI
39	5420–5460	0.02	TiO ; FeI ; MnI
40	5460–5516	0.02	MgH ; TiO ; C_2 ; MnI ; CN
41	5516–5562	0.01	MgH ; CaOH ; C_2 ; MgI ; MnI
42	5562–5630	0.01	MgH ; FeI ; CaI ; TiO ; C_2 ; CN
43	5630–5676	0.01	TiO ; C_2 ; FeI
44	5676–5726	0.02	TiO ; NaI ; MgI ; FeI
45	5726–5800	0.02	TiO ; CN ; FeI
46	5800–5848	0.00	TiO
47	5848–5880	0.01	TiO ; CN ; TiI ; HeI ; CaI
48	5880–5914	0.07	NaI ; TiO ; TiI
49	5914–5950	0.03	TiO ; C_2 ; TiI ; FeI
50	5950–6002	0.02	TiO ; CN ; C_2
51	6002–6056	0.01	TiO ; CaOH ; C_2 ; FeI
52	6056–6108	0.01	TiO ; MgH ; CaI ; FeI
53	6108–6156	0.03	CN ; C_2 ; FeI ; TiO
54	6156–6210	0.05	TiO ; CaI ; C_2 ; CN ; FeI
55	6210–6274	0.06	TiO ; FeI
56	6274–6322	0.06	TiO ; FeI ; CN

Table 2 (continued)

#	Δλ(Å)	W/Δλ	ABSORBERS
57	6322–6386	0.03	TiO ; CaH ; FeI ; CN
58	6386–6474	0.02	TiO ; CaI ; FeI ; CN
59	6474–6540	0.04	FeI ; BaII ; CaI ; TiO ; CN
60	6540–6586	0.06	Hα ; TiO ; FeI
61	6586–6670	0.02	TiO ; FeI ; CN
62	6670–6736	0.02	TiO ; CaI ; FeI
63	6736–6858	0.02	TiO ; CN ; FeI ; CaH
64	6858–6934	0.09	Atmospheric O_2
65	6934–7050	0.02	CaH ; CN ; FeI
66	7050–7158	0.03	TiO ; CN ; CaI ; FeI ; HeI ; NiI
67	7158–7274	0.09	TiO+Atmospheric H_2O
68	7274–7464	0.03	TiO ; VO ; CN ; FeI
69	7464–7580	0.01	CaH ; FeI
70	7580–7690	0.29	Atmospheric O_2

differences between the velocity dispersion of the clusters and that of the considered subsystems within the galaxies.

The choice of the windows was based on the following criteria:

(i) isolation of the strong, easily identifiable features,

(ii) use of absorption features in common among spectra from clusters in a broad range of age and metallicity,

(iii) cross comparison of features both present in various age-metallicity cluster groups and in nuclei of galaxies.

The latter spectra will be presented and population synthesized in a future paper.

We have listed in Table 2, the window limits and the most probable contributors, which, in some cases may become negligible due to age or metallicity differences. A search was made for all features so far used in stellar population synthesis based on spectral characteristics (de Vaucouleurs and de Vaucouleurs, 1959; Alloin et al., 1971; Joly and Andrillat, 1973; O'Connell, 1976; Williams, 1976; Turnrose, 1976; Pritchet, 1977). A number of features or blends, not included in previous studies, especially between 5000 and 7500 Å, were assigned an identification through stellar spectra analysis of different spectral types (Gahm, 1970; Strom et al., 1971; Fäy et al., 1974). The limits of the windows represent a compromise between the width of the absorption as seen on the spectra and the isolation of selected groupings of atomic lines and/or molecular bands. As can be seen in Table 2, most of the weak absorption features, mainly redward of 5000 Å, seen on spectra from clusters of all ages (Fig. 3) are molecular bands arising in low temperature stars (Fäy et al., 1974). Thus, red stars provide an important contribution to the optical light, not only in intermediate or old objects, but also in quite young clusters such as NGC 2004, via the presence of red supergiants.

In column 3 of Table 2, we provide the ratio between the mean equivalent width measured in all clusters for a particular window and the width of this window (excluding H II regions). This parameter represents the mean detection level of the absorption feature or blend. Windows with a 2% level or less, correspond in general, to flux maxima defining continuum points for clusters of any age or metallicity. Windows with a 3% or 4% level, include features which are definitely present in most spectra but cannot be measured accurately, owing to their weakness. The complete set of equivalent width measurements for all windows is presented elsewhere (Bica and Alloin, 1986a). We discuss below conspicuous results regarding some of the windows.

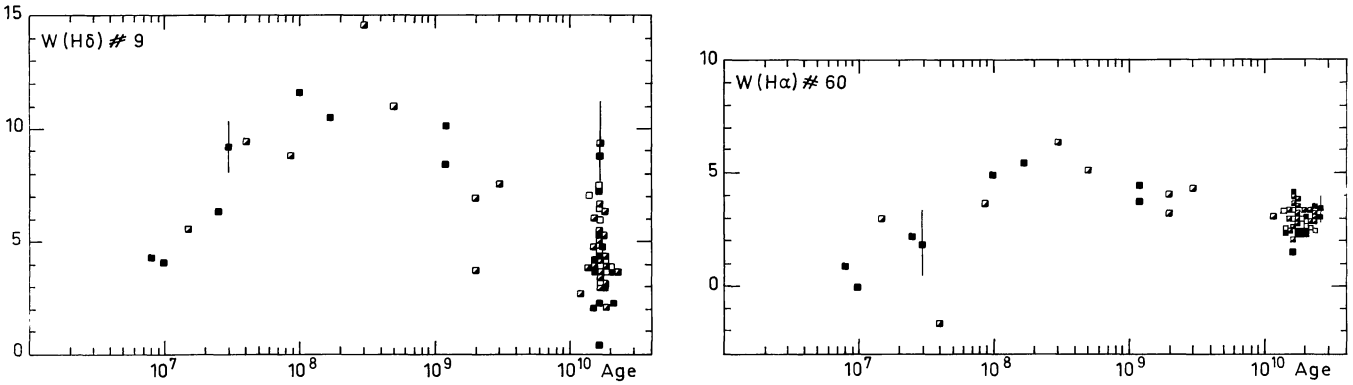

Fig. 4a and b. $W(H\delta)$ and $W(H\alpha)$ respectively, as a function of age. Empty squares correspond to a metallicity less than -1.5; semi-empty ones to the metallicity range $-1.5 \leqq [Z/Z_\odot] \leqq -0.75$; filled squares to a metallicity larger than -0.75

In Fig. 4a, we have plotted $W(H\delta)$ as a function of age. The larger values occur for ages around 4 10^8 yr, where the turn-off point at A stars dominates the integrated spectrum of clusters like NGC 1831 and NGC 1868. The observed $W(H\delta)$ for old metal-poor clusters overlap with those measured in clusters younger than 5 10^7 yr. The metallicity effects are weak or undetectable within the error bars. The lines $H\gamma$ and $H\beta$ present a similar behaviour. This holds true for $W(H\alpha)$ (Fig. 4b), in spite of the fact that the underlying continuum is dominated, then, by late type stars which essentially do not contribute to the line absorption. Due to the latter effect, the W values for $H\alpha$ are much smaller than those of other Balmer lines in the integrated spectrum of star clusters. We emphasize that emission plays no role in this matter because it is present or suspected only in very young clusters. Thus, an absorption Balmer decrement hypothesis for an underlying stellar population cannot be used to disentangle absorption from emission components in nuclei of galaxies.

We have plotted the equivalent widths of metallic lines or molecular bands as a function of metallicity in Figs. 5a through 5i, in an increasing wavelength order. The isochrone defined by the Galactic globular clusters in each plot shows a clear relationship between W of the feature and $[Z/Z_\odot]$. The same behaviour is observed for metallic lines and molecular bands, with the exception that the latter one is more often subject to departures from linearity (Sect. 5). The intermediate age clusters are, in some cases undistinguishable from the globular clusters and eventual drifts are systematically towards the sequence defined by the young blue clusters. The wavelength succession of the figures shows how younger turn-off points affect the equivalent width of metallic features. Indeed, the enhancement of the blue continuum, due to the upper main sequence stars, splits the W vs. $[Z/Z_\odot]$ plots into several loci dependent on the age. On the contrary, the W vs. metallicity relationship for features in the red tends to be more single-valued: in the Mg I + MgH plot, the isochrones defined by Galactic globular clusters and by young clusters are closer to each other and the sets of points even completely overlap for TiO bands.

The interstellar component of the Na I absorption, especially for highly reddened globular clusters, is responsible for most of the dispersion in Fig. 5h. A detailed study of the interstellar Na I as a function of $E(B-V)$ is given elsewhere (Bica and Alloin, 1986b).

In Fig. 6, we have displayed W (Ca II H + Hε) as a function of metallicity. A comparison with Ca II K (Fig. 5a) shows that the strength of this blend is ruled by metallicity, except for the blue clusters about 4 10^8 yr old in which, obviously, Hε contributes much to W (Ca II H + Hε). The windows corresponding to H8, H9, and H10, also strongly blended with metallic features, are likewise metal dominated.

We show in Fig. 7, the continuum slope as measured by e.g. the ratio of the fluxes at λ4020 and λ6630 Å, as a function of age. On the contrary to the W vs. age relationship for $H\delta$ through $H\alpha$, the values for young blue clusters do not overlap with those of old metal poor globular clusters. The effects of metallicity differences are obvious in the globular cluster sample where metal rich objects present steeper spectra resulting from the blanketing effect and a lack of BHB stars. The shape of the curve around 10^8 yr represents an age effect as a result of rapid changes in the relative populations of evolved red stars and top main sequence stars. We checked this result by synthesizing the V flux ratio of red ($(B-V)_0 > 0.6$) to blue stars in composite HR diagrams for different age groups of star clusters in the Galactic disc (Mermilliod 1981a, b). These values have been displayed in an inset to Fig. 7. The flux contributions from magnitude intervals corresponding to the lowest main sequence part are negligible even before incompleteness starts to affect the HR diagrams. Not only is such a shape observed for the overall continuum slope, but also for normalized continuum points at various wavelengths (Bica and Alloin, 1986a). The minimum at $\sim$8 10^7 yr in Fig. 7 coincides for C4020/C6630 and B/R, but a small age shift seems to be present towards 10^9 yr. We assign this difference to the difficulty of dating clusters as they approach the blue-red transition, while the determination of ages for blue clusters is quite precise from stellar evolution models (Renzini and Buzzoni, 1985).

The dispersion of the continuum slope in Fig. 7 for ages $t < 2\ 10^7$ yr is due to the combined effects of internal reddening and rapid integrated color variations as a consequence of the evolution of massive stars. Indeed a variable dust content among Magellanic Cloud H II regions is suggested by the observed spread of $H\alpha/H\beta$ ratios (Pagel et al., 1978 and references therein). The internal reddening of NGC 330 is negligible (Carney et al., 1985) and older clusters are expected to be dust free. The strong TiO bands in the integrated spectrum of NGC 2004 indicate an important flux contribution from red supergiants, contrarily to the slightly older clusters NGC 2100 and NGC 330. Also one should keep in mind that, although these clusters are among the most populous for their age range in the MC, their HR diagrams (references in Table 1) indicate that most of the integrated light comes from a small number of luminous stars subject to a rapid evolution.

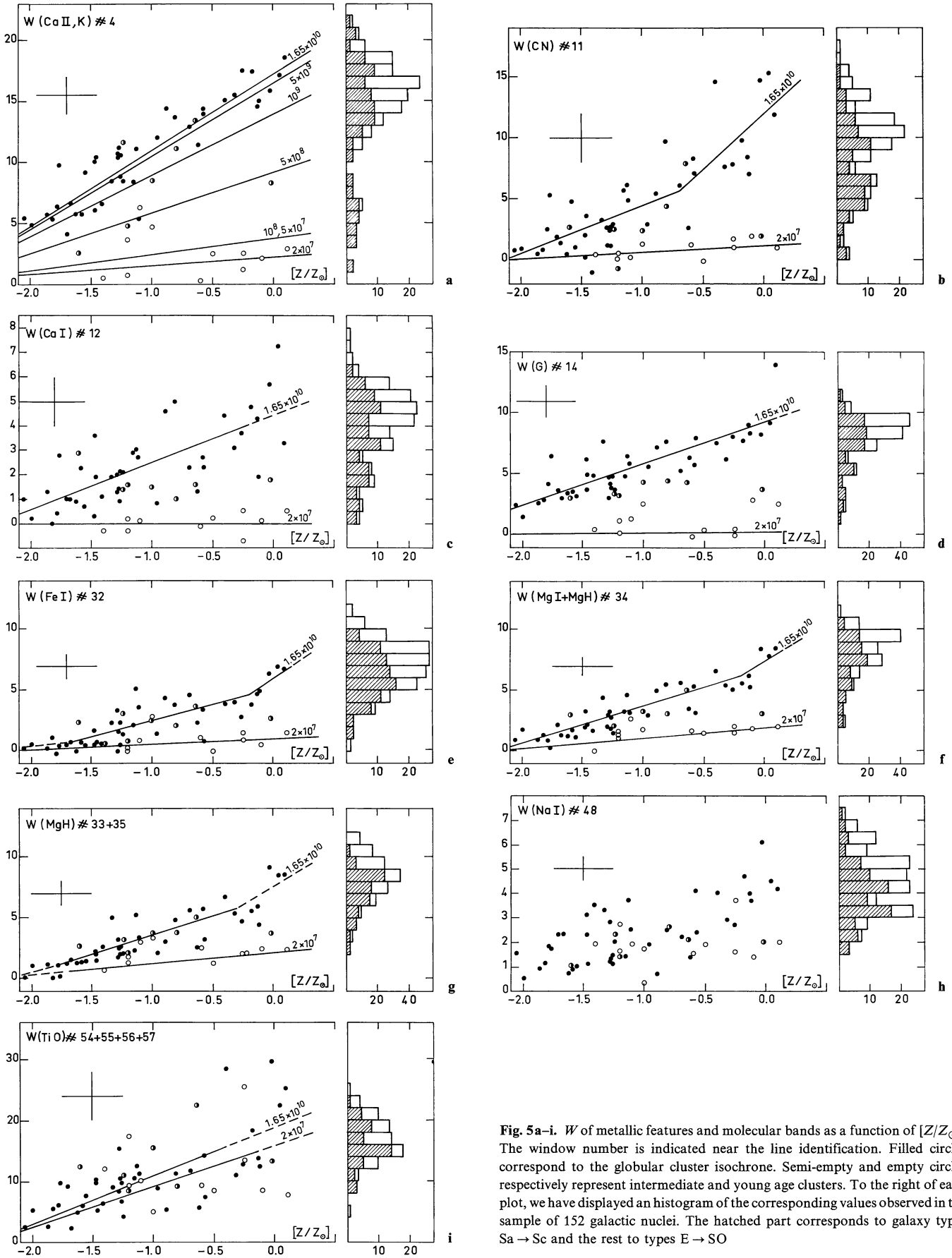

Fig. 5a–i. *W* of metallic features and molecular bands as a function of $[Z/Z_{\odot}]$. The window number is indicated near the line identification. Filled circles correspond to the globular cluster isochrone. Semi-empty and empty circles respectively represent intermediate and young age clusters. To the right of each plot, we have displayed an histogram of the corresponding values observed in the sample of 152 galactic nuclei. The hatched part corresponds to galaxy types Sa → Sc and the rest to types E → SO

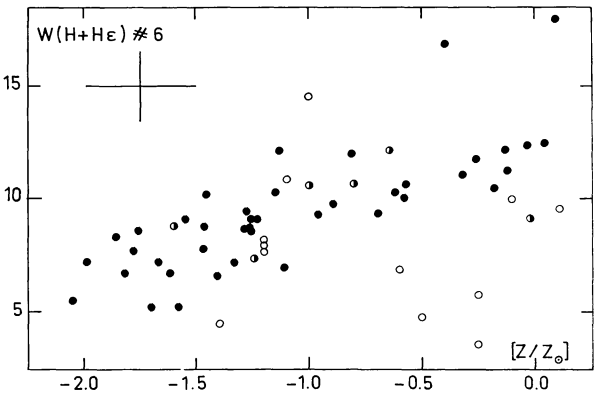

Fig. 6. W (Ca II H+Hε) as a function of $[Z/Z_\odot]$. The symbols are as in Fig. 5

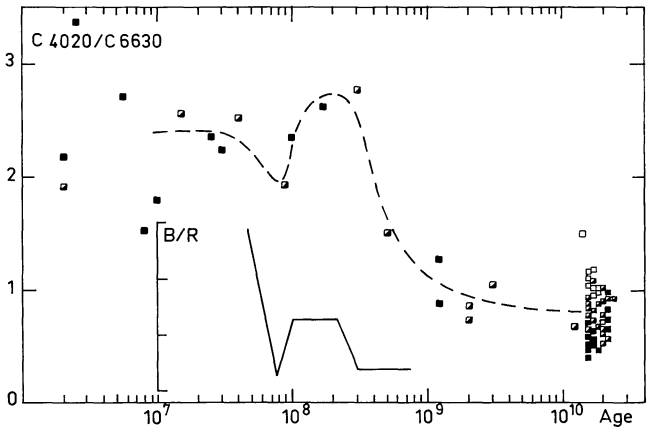

Fig. 7. Variation of the continuum slope with age. The same symbols as in Fig. 4 are used. The inset shows the V flux ratio from the blue to red stellar contributions synthesized from HR diagrams in clusters of different ages

5. Grids of star cluster integrated properties and concluding remarks

The fundamental questions regarding the population synthesis approach undertaken in this paper are as follows:

(i) What is the highest metal content of the stellar populations to be found in nuclear regions of galaxies?

(ii) What is the fraction of galaxies which can be described by the present base reaching up to the solar metallicity?

(iii) How far in $[Z/Z_\odot]$ is it necessary to extrapolate the base properties in order to synthesize populations in the most strong lined galaxies? How valid would such an extrapolation be?

In order to answer these questions, let us consider the results we have recently gathered on 152 normal nuclei in galaxies of morphological types E through Sc, in the luminosity interval $-23.3 < M_B < -16.6$. The spectra, which were obtained and reduced in conditions similar to those of the star clusters, will be presented in a forthcoming paper. They were rebinned to zero redshift, corrected for Galactic reddening, while continuum and equivalent width measurements were made through the same windows. For each metallic window in Fig. 5, we show an inset to the right, containing the histogram of the W values measured in galaxies. Giving more weight to metallic features in the red which are less biased regarding age effects (Sect. 4), no extrapolation at all is needed to describe 50% of the objects and an extrapolation to $[Z/Z_\odot] = 0.6$ is required to describe essentially the entire galaxy sample. Metallicity estimates in early-type galaxies lead to maximum $[Z/Z_\odot]$ values around 0.3 (e.g. Aaronson et al., 1978) and 0.3–0.5 (Pickles, 1985). Moreover, the present result, derived from absorption lines only, is in fair agreement with oxygen abundances in central H II regions of spiral galaxies (Pagel and Edmunds, 1984). The $[O/O_\odot]$ values for the gas imply that the present metal content in the most metal rich stellar generation in the nuclei of spiral galaxies is at most a factor 4 higher than solar. Moreover, 50% of galaxies in their sample (highly peaked at $-22 < M_B < -21$) could be population synthesized with a solar metallicity base. The required 0.6 dex extrapolation of the cluster base properties corresponds to 20% of the observed $[Z/Z_\odot]$ interval. It is important to note that the globular cluster scale has been recently calibrated up to the solar abundance through observations of individual stars in NGC 5927 (Cohen, 1983). Together with NGC 5927, we have also observed NGC 6528, NGC 6440 and NGC 6553, some of the most metal-rich globular clusters in the Galaxy, according to intermediate band photometry (Bica and Pastoriza, 1983; Zinn and West, 1984). Indeed, the integrated spectra of these three clusters are clearly more strong-lined than that of NGC 5927.

Metallicity indices in the optical (Faber, 1973; Burstein et al., 1984) as well as in the infrared (Frogel et al., 1978: Aaronson et al., 1978), indicated that the metal rich globular clusters were considerably more metal-poor than the major part of luminous galaxies. In fact, the most metal-rich clusters in the former optical and infrared samples (respectively NGC 6356 and NGC 6637) are a factor 4 to 6 more metal poor than the sun. In Fig. 8, the gap between NGC 6356 and, for example, one of the strongest-lined galaxies, the giant early-type Virgo member NGC 4649, is filled in the present sample by the very metal-rich globular cluster NGC 6440.

According to Fig. 5, the pure metallic features present a remarkable W vs. metallicity relationship, both for the well defined globular cluster isochrone and the young blue cluster sequence. A clear departure from linearity is present for the metal rich globular clusters in the CN band (#11). A similar effect has been observed in M31 globulars (Burstein et al., 1984). The windows #32 to #35, which contain an important contribution from MgH and C_2, also present a slight departure from linearity. Possibly TiO does so.

In view of population synthesis, we wish to derive a grid of star cluster properties covering the whole age-metallicity plane with a suitable step. Therefore, we have for each feature, defined the extreme relations (W, metallicity) for the globular cluster and young cluster isochrones (taking into account only clusters younger than $5\ 10^7$ yr and excluding H II regions). These relations systematically converge at low metallicities: linear regressions for the 5 more significant features led to a zero-point $[Z/Z_\odot] = -2.45 \pm 0.35$ which was subsequently used as a reference point. The mean age within each group was assigned to the isochrone. The age interpolation has been weighted by the continuum slope vs. age relationship (Fig. 7). On top of Fig. 5, we have drawn the two extreme relations (globular and young clusters) and, in the case of Ca II K some intermediate ones as well. The grid predictions to be used in future stellar population synthesis is presented elsewhere (Bica and Alloin, 1986a). The mean properties of star clusters, having $-2.0 \leqq [Z/Z_\odot] \leqq 0$, with an 0.5 dex step as well as the extrapolated value at $[Z/Z_\odot] = 0.6$, and with ages $1.65\ 10^{10}$ yr, $5\ 10^9$ yr, 10^9 yr, $5\ 10^8$ yr, 10^8 yr, $5\ 10^7$ yr, 10^7 yr have been interpolated for this purpose.

The main conclusions of the present work are the following:

(i) Integrated spectra of 63 star clusters provide a useful base for population synthesis in galaxies.

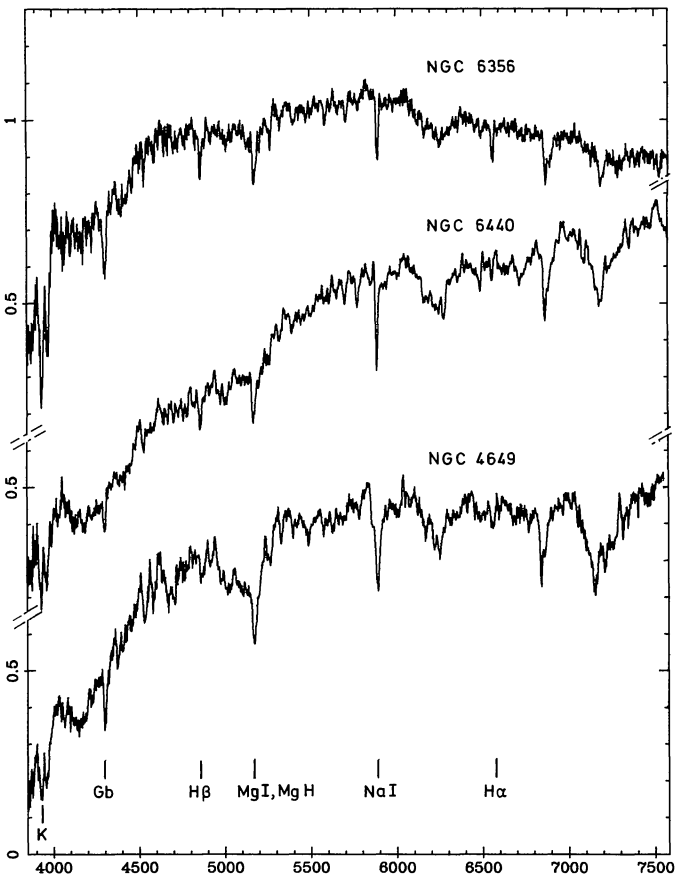

Fig. 8. Spectra of one of the most metal rich globular clusters in our sample (NGC 6440), a cluster (NGC 6356) considered metal-rich in previous comparisons with galaxies and NGC 4649, a very strong-lined early-type galaxy

(ii) A number of weak absorption features from 3780 to 7690, mostly arising from molecular bands in late-type star atmospheres, are present not only in red clusters but also in young ones via red supergiant stars.

(iii) As a consequence of the low dispersion we used, many trustworthy maxima led to a good estimation of the continuum level.

(iv) About 30 out of the 70 windows we defined present features at a significant level for being used in stellar population synthesis.

(v) We show the influence of younger turn-off points on W for metallic features and molecular bands. The enhancement of the blue continuum due to upper main sequence stars, defines, in the W vs. $[Z/Z_\odot]$ plots, several loci depending on the age. On the contrary, the W vs. $[Z/Z_\odot]$ relations in the case of red features tend to be single-valued, regardless of age.

(vi) Metallic lines and molecular bands present a similar behaviour as a function of $[Z/Z_\odot]$, the latter more often departing from linearity for large $[Z/Z_\odot]$.

(vii) The lines Hα to Hδ show the same dependence on age with maximum values at around 4 10^8 yr. For a given age, W(Hα) is always smaller than the three next Balmer lines because the underlying continuum is dominated by late type stars which essentially do not contribute to the line absorption. Thus it is not possible to assume a Balmer absorption decrement in the underlying stellar populations for disentangling emission from absorption components in galaxies.

(viii) The lines Hε through H10, strongly blended with metallic features, present a metal-dominated behaviour.

(ix) The continuum distribution differences and not the Balmer line equivalent widths allow one to distinguish between young populations and old metal-poor ones in galaxies.

(x) The comparison of W for metallic features in 152 normal galactic nuclei and in the cluster base shows that around 50% of the galaxy sample can be population synthesized without extrapolation of the cluster base properties. An extrapolation to $[Z/Z_\odot] = 0.6$ is required to describe essentially the whole sample.

Acknowledgements. We are gratefully indebted to the ESO staff, both at La Silla and Garching as well as to the computer center groups in Meudon Observatory and at the Institut d'Astrophysique. We acknowledge interesting comments and suggestions from B. Pagel. Eduardo Bica thanks the Brazilian Institution CNPq, for a fellowship.

References

Aaronson, M., Cohen, J., Mould, J., Malkan, M.: 1978, *Astrophys. J.* **223**, 824
Aaronson, M., Frogel, J.A., Persson, S.: 1978, *Astrophys. J.* **220**, 442
Alloin, D., Andrillat, Y., Souffrin, S.: 1971, *Astron. Astrophys.* **10**, 401
Arp, H., Cuffey, J.: 1962, *Astrophys. J.* **136**, 51
Barbaro, G., Dallaporta, N., Fabri, G.: 1961, *Astrophys. Space Sci.* **3**, 123
Becker, S., Mathews, G.: 1983, *Astrophys. J.* **270**, 155
Bica, E., Alloin, D.: 1986a, *Astron. Astrophys. Suppl. Ser.* (in press)
Bica, E., Alloin, D.: 1986b, *Astron. Astrophys.* (in press)
Bica, E., Pastoriza, M.: 1983, *Astrophys. Space Sci.* **91**, 99
Boeshaar, G., Boeshaar, P., Czyzak, S., Aller, L., Lasker, B.: 1980, *Astrophys. Space Sci.* **68**, 335
Burstein, D., Faber, S.M., Gaskell, C.M., Krumm, N.: 1984, *Astrophys. J.* **287**, 586
Carney, B., Janes, K., Flower, P.: 1985, *Astron. J.* **90**, 1196
Christian, C., Heasley, J., Janes, K.: 1985, *Astrophys. J.* **299**, 683
Ciani, A., d'Odorico, S., Benvenuti, P.: 1984, *Astron. Astrophys.* **137**, 223
Cohen, J.G.: 1982, *Astrophys. J.* **258**, 143
Cohen, J.G.: 1983, *Astrophys. J.* **270**, 654
Cowley, A., Hartwick, F.: 1982, *Astrophys. J.* **259**, 89
de Vaucouleurs, G., de Vaucouleurs, A.: 1959, *Publ. Astron. Soc. Pacific* **71**, 83
Dottori, H.: 1981, *Astrophys. Space Sci.* **80**, 267
Dottori, H., Bica, E.: 1981, *Astron. Astrophys.* **102**, 245
Dottori, H., Pastoriza, M., Bica, E.: 1983, *Astrophys. Space Sci.* **91**, 79
Durand, D., Hardy, E., Melnick, J.: 1984, *Astrophys. J.* **283**, 552
Dufour, R., Harlow, W.V.: 1977, *Astrophys. J.* **216**, 706
Faber, S.M.: 1972, *Astron. Astrophys.* **20**, 361
Faber, S.M.: 1973, *Astrophys. J.* **179**, 731
Fäy, T.D., Stein, W.L., Warren, W.H.: 1974, *Publ. Astron. Soc. Pacific* **86**, 772
Frogel, J., Persson, S., Aaronson, M., Matthews, K.: 1978, *Astrophys. J.* **220**, 75
Gahm, G.F.: 1970, *Astron. Astrophys.* **4**, 268
Hartwick, F.D., Hesser, J.E.: 1973, *Astrophys. J.* **183**, 883
Hodge, P.W.: 1982, *Astrophys. J.* **256**, 447
Hodge, P.W.: 1983, *Astrophys. J.* **264**, 470
Hodge, P.W.: 1984a, IAU *Symp.* **108**, p. 7

Hodge, P.W.: 1984b, *Publ. Astron. Soc. Pacific* **96**, 947
Hodge, P.W., Lee, S.O.: 1984, *Astrophys. J.* **276**, 509
Janes, K.A.: 1979, *Astrophys. J. Suppl.* **39**, 135
Janes, K.A., Demarque, P.: 1983, *Astrophys. J.* **264**, 206
Joly, M., Andrillat, Y.: 1973, *Astron. Astrophys.* **26**, 95
Mermilliod, J.C.: 1981a, *Astron. Astrophys. Suppl.* **44**, 467
Mermilliod, J.C.: 1981b, *Astron. Astrophys.* **97**, 235
McClure, R.D., Twarog, B.A.: 1978, in *Chemical and Dynamical Evolution of the Galaxy*, eds. E. Basinska-Grezesik, M. Mayor, Torun
Mould, J., Aaronson, M.: 1980, *Astrophys. J.* **240**, 464
Mould, J., Aaronson, M.: 1982, *Astrophys. J.* **263**, 629
Nelson, M., Hodge, P.W.: 1983, *Publ. Astron. Soc. Pacific* **95**, 5
O'Connell, R.W.: 1976, *Astrophys. J.* **206**, 370
Olszewski, E.: 1984, *Astrophys. J.* **284**, 108
Pagel, B.E., Edmunds, M., Fosbury, R., Webster, B.: 1978, *Monthly Notices Roy. Astron. Soc.* **184**, 569
Pagel, B.E., Edmunds, M.G.: 1981, *Ann. Rev. Astron. Astrophys.* **19**, 77
Pagel, B.E., Edmunds, M.G.: 1984, *Monthly Notices Roy. Astron. Soc.* **211**, 507
Pickles A.J.: 1985, *Astrophys. J.* **296**, 340
Pritchet, C.: 1977, *Astrophys. J. Suppl.* **35**, 397
Rabin, D.: 1982, *Astrophys. J.* **261**, 85
Renzini, A., Buzzoni, A.: 1985, in *Spectral Evolution of Galaxies*, eds. C. Chiosi, A. Renzini, Reidel, Dordrecht
Richtler, T., Nelles, B.: 1983, *Astron. Astrophys.* **119**, 75
Searle, L., Wilkinson, A., Bagnuolo, W.G.: 1980, *Astrophys. J.* **239**, 803
Smith, H.: 1984, *Astrophys. J.* **281**, 148
Strom, S.E., Strom, K.M., Corbon, D.F.: 1971, *Astron. Astrophys.* **12**, 177
Turnrose, B.E.: 1976, *Astrophys. J.* **210**, 33
VandenBerg, D.A.: 1983, *Astrophys. J. Suppl.* **51**, 29
Van den Bergh, S.: 1975, *Ann. Rev. Astron. Astrophys.* **13**, 217
Van den Bergh, S.: 1981, *Astron. Astrophys. Suppl.* **46**, 79
Williams, T.B.: 1976, *Astrophys. J.* **209**, 716
Zinn, R., West, M.: 1984, *Astrophys. J. Suppl.* **55**, 45

Note added in proof: A very recent paper (Christian et al.) discusses in detail the Galactic open cluster NGC 2158. The best fit parameters found in that paper are compatible with our compilation in Table 1, except for a slightly older age (3 Gyr instead of 1.2 Gyr). Indeed, this new value is in better agreement with the locus of the cluster in our Figures.